Speed stiffness characteristics of electro-hydro-mechanical system

Qingqing Tian*, Lichen Gu

School of Mechanical and Electronic Engineering, Xi'an University of Architecture and Technology, Xi'an, 710055, China

Corresponding Author Email: tianqing12345@126.com

ABSTRACT

This paper aims to enhance the speed stiffness of the electro-hydro-mechanical system (EHMS). Focusing on the variable speed pump-controlled hydraulic motor system (VSPCMS), a typical EHMS, a mathematical model was established to discuss the coupling mechanism between multiple system parameters under the load condition, the physical meaning of system speed stiffness was explained, and the law of speed stiffness was disclosed under the action of multi-source variables. Moreover, several experiments were carried out to explore how the system speed stiffness is affected by three leading influencing factors in the VSPCMS, hydraulic motor displacement, leakage coefficient (system temperature and pressure) and motor shaft inertia. The experimental data agree well with the theoretical results: the system speed stiffness is positively correlated with hydraulic motor displacement and hydraulic motor shaft inertia and negatively with leakage coefficient. The research findings lay a theoretical basis for enhancing system speed stability, reducing speed fluctuations and optimizing system design.

1. INTRODUCTION

With simple structure, easy control and low noise, the electro-hydro-mechanical system (EHMS) has been extensively applied in such fields as aerospace engineering, precision machining and construction machinery. A typical example of the EHMS is the variable speed pump-controlled hydraulic motor system (VSPCMS). This system offers an ideal solution to elevators and injection moulding machines, thanks to its global power matching [1-2]. With the development of modern industry, stricter requirements are now being imposed on the operation of mechanical equipment. This calls for deep exploration into the performance of the VSPCMS.

The operation of the VSPCMS directly hinges on the speed stiffness, an indicator of the system's ability to output a stable speed against the load change. As the combined effect of multiple system parameters, this indicator reveals many working conditions of the system, including flow fluctuations, electric motor features, oil-liquid compression, hydraulic pump/motor oil leak and shaft load, and induces changes to system operation. For better application of the VSPCMS, it is meaningful to discuss and disclose the law of speed stiffness.

Signals, such as vibration, flow, pressure and so on, are the common performance evaluation indicators. These signals are effective for component performance evaluation. Due to the change of working conditions and operating parameters, these signals are submerged in strong vibration or noise signal. So there are some limitations in using these single signals as system performance evaluation indicators. Whereas the speed stiffness is proved to an effective indicator to evaluate the system [1-3].

In general, the VSPCMS is featured by a poor speed stiffness. The existing studies on this system mainly concentrate on the design of hydraulic motor speed controller and control algorithm [6-10], or the stiffness of a subsystem of the MEHS [11-12]. There are few systematic reports on the theories of the speed stiffness of the VSPCMS. To make up for the gap, this paper analyses the multiparameter coupling mechanism of the VSPCMS, a typical EHMS, discloses the physical meaning of the system speed stiffness, and investigates the law of speed stiffness under the action of multi-source variables. The research findings lay a theoretical basis for enhancing system speed stability, reducing speed fluctuations and optimizing system design.

The remainder of this paper is organized as follows: Section 2 analyses the multiparameter coupling mechanism of the VSPCMS; Section 3 introduces a method for discussing the speed stiffness of the VSPCMS; Section 4 verifies the method through experiments and analyses the experimental results; Section 5 wraps up this paper with several meaningful conclusions.

2. MULTIPARAMETER COUPLING MECHANISM

According to the simplified model in Figure 1, the VSPCMS consists of three subsystems, namely, the electric motor-hydraulic pump subsystem, the hydraulic pump-hydraulic motor subsystem, and the hydraulic motor-load subsystem.

The following assumptions were put forward for subsequent analysis:

(1) The leakage of the hydraulic pump and the hydraulic motor flows in a laminar pattern.

(2) The pressure loss in the pipe between the hydraulic pump and the hydraulic motor is negligible.

(3) The flow pulsation of the oil supply by the hydraulic pump is not considered.

(4) There is no elastic load (A servo system is mainly

subjected to the inertial load, with no or a negligible amount of elastic load. This is particularly true for a servo system containing a hydraulic motor).
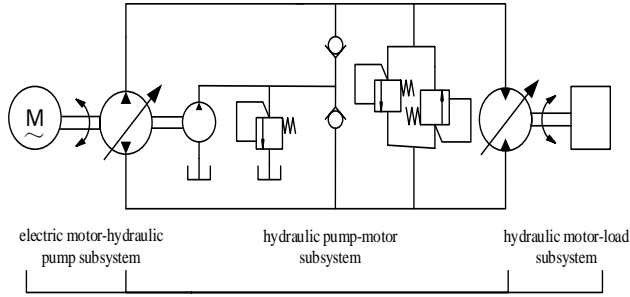

Figure 1. Simplified model of the VSPCMS

The multiparameter coupling of the VSPCMS (Figure 1) can be described by a set of differential equations of its three subsystems [13-16, 19]:

(1) Electric motor-hydraulic pump subsystem:

$$\frac{n\omega_s L_M^2}{L_R(1+T_r s)}i_{sM}^2 - B_e\omega_e - D_p(p-p_r) = J_e\frac{d\omega_e}{dt} \tag{1}$$

where n is the number of pole pairs of the electric motor; ω_s and ω_e are the synchronous speed and shaft speed of the electric motor, respectively; L_M and L_R are the mutual inductance of the three-phase stator winding and the self-inductance of the three-phase rotor winding of the electric motor, respectively; T_r is the rotor time constant; s is the differential operator; i_{sM} is the stator current excitation component; p and p_r are the high-pressure pipe pressure and charge pressure of low-pressure pipe in the of the hydraulic system, respectively; D_p is the displacement of the hydraulic pump; B_e is the viscous damping coefficient of the output shaft in the electric motor; J_e is the total inertia of the electric motor and the pump (converted to that on the electric motor shaft).

Through Laplace transform, Eq (1) can be rewritten as:

$$\frac{n\omega_s L_M^2}{L_R(1+T_r s)}i_{sM}^2 - B_e\omega_e - D_p P = J_e s\omega_e \tag{1a}$$

(2) Hydraulic pump- hydraulic motor subsystem

$$D_p\omega_p - C_{ip}(p-p_r) - C_{ep}p = \frac{V_0}{\beta_e}\frac{dp}{dt} + C_{im}(p-p_r) + C_{em}p + D_m\omega_m \tag{2}$$

where D_m is the displacement of the hydraulic motor; C_{ip} and C_{ep} are the internal and external leakage coefficients of the hydraulic pump, respectively; C_{im} and C_{em} are the internal and external leakage coefficients of the hydraulic motor, respectively; ω_p and ω_m are the shaft speeds of the hydraulic pump and the hydraulic motor, respectively; V_0 is the volume of the chamber (including a working chamber, a non-working chamber, and the connecting pipe between the two chambers of the hydraulic pump and the hydraulic motor); β_e is the bulk elastic modulus of oil.

Note that the viscosity of hydraulic oil may change with the temperature and pressure, leading to varying leakage rate of the hydraulic pump and hydraulic motor, which, in turn, affects the output flow of the pump and the input flow of the

hydraulic motor. Therefore, the temperature and pressure must be compensated, that is, the leakage coefficients of the hydraulic pump and motor must be corrected [17, 20-21]. Here, the Vogel equation on viscosity-temperature relation is introduced:

$$\mu_0 = a \cdot e^{\frac{b}{T+c}} \tag{3}$$

where μ_0 is the dynamic viscosity of hydraulic oil at a given temperature under one bar; a, b and c are the coefficients associated with the hydraulic oil; T is the oil temperature.

When the pressure is greater than 5MPa, the effect of pressure on the viscosity must be considered. The relation between viscosity and pressure satisfies the Barus equation:

$$\mu = \mu_0 \cdot e^{\lambda p} \tag{4}$$

where μ is the dynamic viscosity of the oil; λ is the pressure-viscosity coefficient.

Considering the pressure, temperature and working condition, the dynamic leakage coefficient of the pump can be expressed as:

$$C_t^{'} = k \cdot C_t \Bigg/ \left(a \cdot e^{\frac{b}{T+c} + \lambda p} \right) \tag{5}$$

where k is the fuzzy compensation coefficient of working condition; C_t ($C_t = C_{ip} + C_{ep} + C_{im} + C_{em}$) is the total leakage coefficient.

Considering the dynamic leakage coefficient, Eq (2) can be rewritten as follows through Laplace transform:

$$D_p\omega_p = \frac{V_0}{\beta_e}sP + C_t^{'}P + D_m\omega_m \tag{2a}$$

(3) Hydraulic motor-load subsystem

$$D_m(p-p_r) = J_m\frac{d\omega_m}{dt} + B_m\omega_m + T_L \tag{6}$$

where J_m is the total inertia of the hydraulic motor and the load (converted to that on the shaft of the hydraulic motor); B_m is the viscous damping coefficient of the output shaft of the hydraulic motor; T_L is the load moment acting on the shaft of the hydraulic motor.

Through Laplace transform, Eq (6) can be rewritten as:

$$D_m P = J_m s\omega_m + B_m\omega_m + T_L \tag{6a}$$

Removing intermediate variables P and ω_e (ω_p) in Eq (1a), (2a) and (6a), we have:

$$\omega_m = \frac{D_p \cdot D_m \dfrac{n\omega_s L_M^2}{L_R(1+T_r s)}i_{sM}^2 - \left[D_p^2 + (J_e s + B_e)\left(C_t^{'} + \dfrac{V_0}{\beta_e}s\right) \right]T_L}{D_p^2 \cdot (J_m s + B_m) + (J_e s + B_e)\left(C_t^{'} + \dfrac{V_0}{\beta_e}s\right)(J_m s + B_m) + (J_e s + B_e)\cdot D_m^2} \tag{7}$$

Eq (7) shows that the conversion between the mechanical, electrical and hydraulic energies of the VSPCMS changes with any internal parameter of the system (e.g. the displacement of the hydraulic pump, the displacement of the hydraulic motor, the leakage coefficient, and bulk elastic modulus of the oil). In this case, the system output ω_m will undergo changes until reaching a new state of equilibrium. Under the new state, the other internal parameters of the system will also change. This process is called multiparameter coupling.

3. SPEED STIFFNESS ANALYSIS

The speed stiffness illustrates the impact of the load disturbance torque T_L on the output speed ω_m of the hydraulic motor. In the VSPCMS, the speed stiffness reflects the ability of the system to output a stable speed against load changes. According to Eq (7), the dynamic speed stiffness features of the system can be obtained as:

$$\frac{T_L}{\omega_n} = -\left[\left(J_m s + B_m\right) + \frac{\left(J_e s + B_e\right) \cdot D_m^2}{D_p^2 + \left(J_e s + B_e\right)\left(C_t' + \frac{V_0}{\beta_e}s\right)} \right] \tag{8}$$

Eq (8) shows that the speed stiffness of the system is the result of the coupling between multiple system parameters. The value of the speed stiffness is mainly affected by the displacement of the hydraulic pump and motor, the rotational inertia of subsystem, the viscous damping coefficient, the leakage coefficient of the hydraulic system, and the bulk elasticity module of the oil. The symbol in Eq (8) reveals negative correlation between the load torque and the system output speed.

The relationships between the dynamic speed stiffness and the multiple parameters are as follows: the speed stiffness is positively correlated with the leakage coefficient, the load inertia and the displacement of the hydraulic motor, and negatively with the displacement of the hydraulic pump. The variation in the load conditions is bound to cause changes to the internal parameters of the system. Thus, the speed stiffness of the system must change dynamically with the working condition. The stronger the speed stiffness, the stronger the system's resistance to impact and disturbance and the more stable the system output.

The real-time and no-load shaft speeds and torques of the hydraulic motor (hereinafter referred to as the experimental data) are denoted as $\{\omega_m, T_L\}$ and $\{\omega_{m0}, T_{L0}\}$, respectively. Then, the speed stiffness can be expressed as [18, 22]:

$$G = \left| \frac{T_L - T_{L0}}{\omega_m - \omega_{m0}} \right| \tag{9}$$

4. EXPERIMENTAL VERIFICATION

Figure 2 is the schematic diagram of the VSPCMS. Specifically, the permanent-magnet synchronous motor (PMSM) 13 controls the hydraulic motor speed together with the servo controller 18. The current converter 7 converts the control voltage into control current signals. The signals determine the output torque of magnetic powder brake 6 on the piston motor 3. Besides, different number of inertia disks can be added to the hydraulic motor shaft to simulate different load inertia conditions. The output shaft of the hydraulic motor has a speedometer disc 4 and a magneto-electric tachometric transducer 8. The disc and the transducer work together to measure the hydraulic motor speed. In addition, the system boasts several sensors of flow, pressure and temperature. The signal captured by each sensor is transferred via the Advantech data collection system to the industrial computer 20 (language environment: LabVIEW) for processing. And the main experimental components and parameters are shown in Table 1.
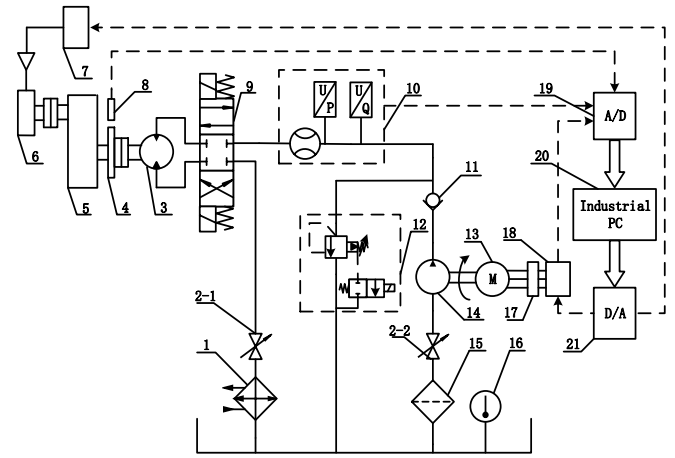

Figure 2. Schematic diagram of the VSPCMS (1. Radiator; 2-1, 2-2 Stop valves; 3. Piston motor; 4. Speedometer disc; 5. Reducer; 6. Magnetic powder brake; 7. Current converter; 8. Magneto-electric tachometric transducer; 9. Solenoid directional valve; 10. Pressure and flow sensor; 11. Check valve; 12. Electromagnetic relief valve; 13. Permanent-magnet synchronous motor; 14. Gear pump; 15. Oil filter; 16. Temperature sensor; 17. Hall voltage/current sensor; 18. Servo controller; 19. A/D converter; 20. Industrial computer; 21. D/A converter.)

Table 1. Main components and parameters

Components	Parameters
piston motor	4 ~10ml/r manual adjustable displacement
magnetic powder brake	0~100N·m
pressure sensor	Accurate class:0.5%FS; Measuring range:0-25MPa
flow sensor	Accurate class:1.0; Measuring range:0.4~1.2m3/h
Temperature sensor	Accurate class:0.5; Measuring range: -50~100°C
Magneto-electric tachometric transducer	0.3Hz~10kHz

As mentioned before, the system speed stiffness may undergo changes due to the dynamic change of the internal parameters of the system. Hence, hydraulic motor displacement, leakage coefficient and hydraulic motor shaft inertia were selected to discuss their effects on the speed stiffness of the experimental system in Figure 2.

4.1 Hydraulic motor displacement

The experimental data at the hydraulic motor displacements of 6mL/r, 8mL/r and 10mL/r were recorded with zero inertia disc at the electric motor speed of 600 r/min, the oil temperature of 20°C and the magnetic powder brake controlled voltage of 0.55V. The speed stiffness curves of the system are shown in Figure 3.
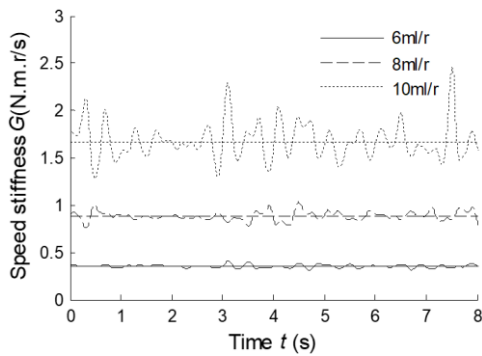

Figure 3. Speed stiffness curves at different hydraulic motor displacement

As shown in Figure 3, the speed stiffness of the system exhibited a significant improve with the increase of the hydraulic motor displacement. This trend is attributable to the decline in the hydraulic motor speed (primary cause: the system speed gain is negatively correlated with hydraulic motor displacement; secondary cause: the displacement increase reduces the system pressure and leakage and the drop of hydraulic motor speed). The relationship between the system speed stiffness and hydraulic motor displacement is given in Figure 4. It can be seen that the two parameters have a quadratic relationship. The fitting curve equation $G = 0.02049 * D_m^2 - 0.4007$, goodness of fit: SSE: 0.001403, R^2: 0.9984, adjusted R^2: 0.9968 and RMSE: 0.03745, which proves the good agreement between the experimental data and the theoretical results.
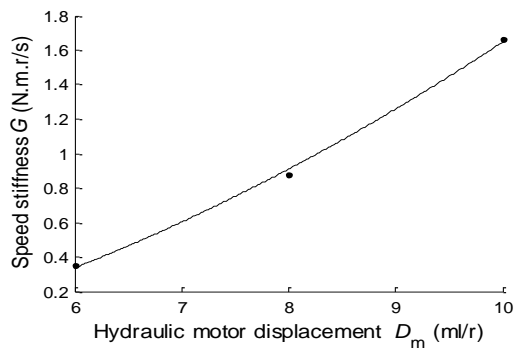

Figure 4. Relationship between speed stiffness and hydraulic motor displacement

4.2 Leakage coefficient

Among system parameters, system temperature and pressure are leading influencing factors on the leakage coefficient. Thus, this subsection aims to disclose their impacts on system speed stiffness.

(1) System temperature

The experimental data at the oil temperatures of 20°C, 27°C and 36°C were recorded with zero inertia disc at the electric motor speed of 600 r/min, the hydraulic motor displacement of 10mL/r and the magnetic powder brake controlled voltage of 0.55V. The speed stiffness curves of the system are shown in Figure 5.
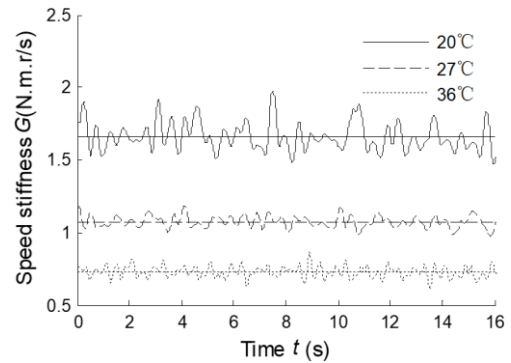

Figure 5. Speed stiffness curves at different temperature

As shown in Figure 5, the motor speed stiffness exhibited a decline trend with the rise in temperature. This is because the dynamic viscosity of the oil decreases with the increase in oil temperature, resulting in a growth of the system leakage coefficient. In this case, the drop of hydraulic motor speed increases, which reduces the system speed stiffness. The experimental data are consistent with the theoretical results.

(2) System pressure

The experimental data as the magnetic powder brake controlled voltage changed along 0V-0.8V-0V were recorded with zero inertia disc at the electric motor speed of 600 r/min, the hydraulic motor displacement of 8mL/r and the oil temperature of 33°C. The speed stiffness curves of the system are shown in Figure 6.
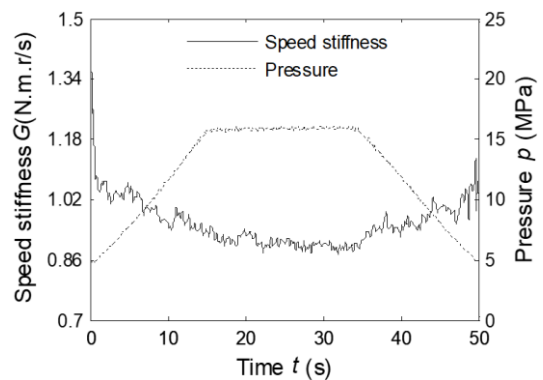

Figure 6. Speed stiffness curves at different pressure

As shown in Figure 6, the system speed stiffness decreased with the increase in system pressure. The main reason is that the dynamic viscosity of the oil decreases with the increase in

system pressure, resulting in a growth of the system leakage coefficient. In this case, the drop of hydraulic motor speed increases, which reduces the system speed stiffness. The experimental data are consistent with the theoretical results.

To sum up, the system speed stiffness decreased with the increase in the leakage coefficient (rising system temperature/pressure). This conclusion agrees well with the theoretical results.

4.3 Hydraulic motor shaft inertia

The experimental data with 0, 1 and 2 inertia discs (each disc weighs 0.6kg • m^2) were recorded at the electric motor speed of 600 r/min, the hydraulic motor displacement of 10mL/r, the oil temperature of 20°C and the magnetic powder brake controlled voltage of 0.55V. The speed stiffness curves of the system are shown in Figure 7.
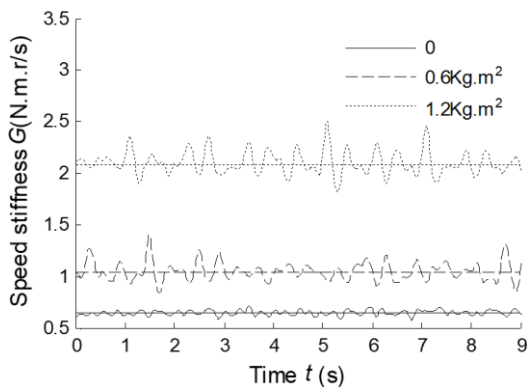

Figure 7. Speed stiffness curves at different hydraulic motor shaft inertia

As shown in Figure 7, the system speed stiffness increased with the rotational inertia on the output shaft of the hydraulic motor. This trend can be explained as follows: With the growth in rotational inertia, when the output flow of the VSPCMS drives the hydraulic motor to work, the first step is to provide energy to the inertia disc(s) to enhance the resistance to load disturbance. That is why the system acquires a greater speed stiffness. The experimental data are consistent with the theoretical results.

5. CONCLUSIONS

In this paper, a mathematical model was established for the VSPCMS and used to study the multiparameter coupling mechanism of the system. On this basis, the author derived the expression for system speed stiffness and determined how it is influenced by multiple parameters. The speed stiffness refers to the system's ability to output a stable speed against the load variation. It is positively correlated with the system's resistance to load disturbance. The greater the speed stiffness, the smaller the fluctuation of output speed and the more stable the system.

Moreover, several experiments were carried out to explore how the system speed stiffness is affected by three leading influencing factors in the VSPCMS, hydraulic motor displacement, leakage coefficient (system temperature and pressure) and hydraulic motor shaft inertia. The experimental data agree well with the theoretical results: the system speed

stiffness is positively correlated with hydraulic motor displacement and hydraulic motor shaft inertia and negatively with leakage coefficient.

The research findings shed new light on system dynamic design and active control. Based on the results on system speed stiffness, the future research will determine the design parameters and control the operation parameters.

REFERENCES

[1] Shimoaki M. (1992). VVVF-controlled hydraulic elevators. Mitsubishi Electric Advance 61(12): 13-15.

[2] Helbig A. (2002). Injection molding machine with electric-hydrostatic drives. The 3rd International Fluid Power Conference, Aachen: Shaker Verlag, 67-82.

[3] Olugbenga MA, Carl DC. (2013). A new active variable stiffness suspension system using a nonlinear energy sink-based controller, vehicle system dynamics. International Journal of Vehicle Mechanics and Mobility, 51(10): 1588-1602.

[4] Jiang WL, Zhu Y, Zheng Z, Zhang S. (2015). Nonlinear vibration mechanism of electro-hydraulic servo system and its experimental verification. Journal of Mechanical Engineering, 51(4): 175-184. https://doi.org/10.3901/JME.2015.04.175.

[5] Chen L, Zhou KK, Li ZX. (2010). Dynamic characteristics fitting of air springs and numerical analysis of air suspensions with variant stiffness. Journal of Mechanical Engineering, 46(4): 93-98. https://doi.org/10.3901/JME.2010.04.093.

[6] Meuser M, Vollmer F. (2003). Using piezo actuators to improve the load stiffness of servo hydraulic drives. Hydraulic and Pneumatic, 47(10): 1-6.

[7] Winnicki A, Olszewski M. (2009). Sliding mode control of electro-hydraulic servo system. Wydawnictwo PAK, 55(3): 174-177.

[8] Wang Y. (2010). Variable structure control for variable pump controlling variable motor. Journal of Beijing University of Aeronautics and Astronautics 36(12):1453-1456. https://doi.org/10.13700/j .bh.1001-5965.2010.12.008

[9] Sun L. (2012). Fuzzy self-tuning PID controller in SEHS. Applied Mechanics and Materials 214: 765-770. DOI: 10.4028/www.scientific.net/AMM.214.765.

[10] Jia YF, Gu LC. (2014). Model and Conditional PID Compensation Control on Flow of Hydraulic Source Driven by Permanent Magnet Servo Motor. Journal of Mechanical Engineering 50(08): 197-204. https://doi.org/10.3901/JME.2014.08.197

[11] Gu HR, Jiao SJ. (2010). Investigation into speed stiffness for milling system of totally-hydraulic milling machine. Chinese Journal of construction machinery 8(1): 14-16, 34. https://doi.org/10.15999/j.cnki.311926.2010.01.008.

[12] Tong W, Liu SD. (2000).The effect of oil contamination on the velocity-load characteristic of the throttle velocity-modulating circuits. Journal of South China

University of Technology (Natural Science Edition) 28(06): 95-99.

[13] Gu LC., Liu PJ., Chen JC. (2011). State recognition technique of hydraulic system based on electrical parameters information fusion. Journal of Mechanical Engineering 47(24): 141-150. https://doi.org/10.3901/JME.2011.24.141

[14] Yang B, Gu LC. (2016). Analysis and on-line measurement method of kinetic energy stiffness for mechanical electro-hydraulic system. 2016 13th International Conference on Ubiquitous Robots and Ambient Intelligence (URAl), China: Xi'an, 604-609.

[15] Manring ND., Luecke GR. (1998). Modeling and designing a hydrostatic transmission with a fixed-displacement motor. Journal of Dynamic Systems, Measurement, and Control 120(1): 45-49.

[16] Kugi A, Schlacher K, Aitzetmuller H, Hirmann G. (2000). Modeling and simulation of a hydrostatic transmission with variable displacement pump. Mathematics and Computers in Simulation 53(4): 409-414.

[17] Gold PW, Schmidt A, Dicke H, Loos J. (2001). Viscosity-pressure-temperature behaviour of mineral and synthetic oils. Journal of Synthetic Lubrication 18(1): 51-79.

[18] Yang B, Gu LC, Liu Y. (2017). A graphical technique of kinetic energy stiffness identification for mechanical electro-hydraulic system. Journal of Vibration and Shock 36(04): 119-126. https://doi.org/10.13465/j.cnki.jvs.2017.04.019.

[19] Sun YG, Qiang HY, Yang KR, Chen QL, Dai GW, Dong M. (2014). Experimental design and development of heave compensation system for marine crane. Mathematical Modelling of Engineering Problems, 1(2): 15-22. https://doi.org/10.18280/mmep.010204

[20] Piancastelli L, Burnelli A, Cassani S. (2017). Validation of a simplified method for the evaluation of pressure and temperature on a RR Merlin XX head. International Journal of Heat and Technology, 35(1): 549-558. https://doi.org/10.18280/ijht.350311

[21] Li J, Yan S, Zhou YH, Yang KX. (2015). Simulations and comparisons of D-section cylinder in the different Re flow. Mathematical Modelling of Engineering Problems, 2(4): 23-28. https://doi.org/10.18280/mmep.020405

[22] Wang TC, Xie YZ, Yan H. (2016). Research of multi sensor information fusion technology based on extension neural network. Mathematical Modelling of Engineering Problems, 3(3): 129-134. https://doi.org/10.18280/mmep.030303